PERFORMANCE OF A GEOFOAM EMBANKMENT AT 100 SOUTH, I-15 RECONSTRUCTION PROJECT, SALT LAKE CITY, UTAH

D. Negussey and A. Stuedlein, Geofoam Research Center, Syracuse University, Syracuse, NY 13244
S. Bartlett, University of Utah, Salt Lake City, Utah
C. Farnsworth, Utah Department of Transportation, Salt Lake City, Utah

ABSTRACT

The Interstate 15 Reconstruction through Salt Lake City, Utah, involved the widening of highway embankments within a North-South corridor and limited right of way. Previous earth embankments over the deep compressive lake deposits have experienced up to 1400 mm of long-term settlement. The Geofoam Research Center and Utah Department of Transportation placed geotechnical instrumentation in portions of Interstate 15 that employed EPS Geofoam to reduce settlement of critical utilities. Construction and post construction stresses and settlements of the embankment were observed. Preliminary results indicate good settlement performance of the geofoam. Total settlements to date of the foundation soils underlying the geofoam and the geofoam are both on the order of 85 mm. The modulus of EPS 20 in the field has been estimated based on observations, and is generally on the order of 10 MPa, suggesting compressive strength testing of 50 mm cube samples in the laboratory provide a severe underestimate of actual modulus values in service. Deformations of geofoam fills due to seating and gap closure take place during construction. Initial indications of long-term settlement suggest the geofoam treated areas will likely settle less than adjoining sections of earth embankment.

KEYWORDS: compression, construction, embankment, geofoam, instrumentation, settlement, soil, utilities

INTRODUCTION

Earlier this year, The Utah Department of Transportation (UDOT) together with Wasatch Constructors finished the $1.6 billion reconstruction of the 27.4 km portion of Interstate 15 (I-15) that runs through Salt Lake City, Utah. The interstate embankment has been widened from eight lanes to ten general-purpose lanes, plus two high occupancy vehicle lanes, within an existing North-South right of way through the middle of the city. The I-15 alignment cuts across an extensive deposit of compressible lake bottom sediments. Much of the area adjacent to the right of way was developed. Acquisition of additional right of way was expensive in some sections. Collateral settlements had to be minimized to prevent damage or disruption of critical utilities, buildings and businesses. The project had to be finished ahead of the 2002 Winter Olympics and the available time to complete the construction was limited. Imposed needs to address these considerations encouraged review and implementation of alternative construction methods such as lime cement columns, staged construction with pre-fabricated vertical wick drains, and the use of expanded polystyrene (EPS) geofoam. Approximately 107,000 m^3 of geofoam has been placed on the I-15 Reconstruction Project, making it the largest application of geofoam to date in the United States (Bartlett, et al (2000)). Construction with geofoam, as opposed to the other more common ground improvement methods, allowed raising and widening of embankment structures without initiating primary consolidation in the underlying clayey soils. Another benefit of EPS geofoam realized by Wasatch Constructors was considerable time savings along fast track or critical path segments. Because geofoam is very light, and the construction procedure with geofoam is simple, skilled labor and specialized equipment was not required.

Along the northern end of the I-15 corridor, critical utility crossings existed beneath the embankment under 100 South. The crossings included 406 mm diameter high-pressure gas line, a 900 mm diameter storm sewer and two 1524 mm diameter fiber optic crossings. Wasatch Constructors identified this crossing to be as a settlement-sensitive area, and widened the embankment with geofoam in both the north and southbound directions. The Geofoam Research Center at Syracuse University, in conjunction with Utah Department Of Transportation (UDOT) and the University of Utah, installed geotechnical instrumentation to monitor the long-term performance of the geofoam

embankment. Background information of the geofoam embankment construction at the 100 South crossing of I-15 and results of the monitoring program to date are presented in this paper.

SUBSURFACE CONDITIONS

The I-15 Corridor lies in the north-central section of the Salt Lake Valley, approximately 20 km east of the Great Salt Lake. The Salt Lake Valley, a 40 km long by 26 km wide basin, is bounded by the Wastach Range to the east, and the Oquirrh Mountains to the west. Quaternary lacustrine deposits are commonly found throughout the valley. Late Pleistocene sediments formed in Lake Bonneville, the Great Salt Lake's predecessor, constitute the dominant soil stratigraphy along the I-15 right of way. Seasonal fluctuations in Lake Bonneville produced thick layers (up to 30 meters) of clays that contain interbed lenses of sandy-silt and sand ranging in thickness from a few millimeters to meters. Subsurface exploration records indicate the sand lenses are generally disconnected and the subsurface drainage is poor. Typically, the near surface layers are desiccated.

Figure 1 shows a CPT soil profile in close proximity to 100 South at I-15. The stratigraphy consists of about 4.5 meters of desiccated clayey silt over 1.5 meters of poorly graded sand. Soft to firm lean varved clay of up to 13.5 meters thickness underlie the poorly graded sand layer. The pertinent soil indices corresponding to the thick clay layer include natural water contents in the range of 20 to 50%, plastic limits in the range of 17 to 30, and liquid limits in the range of 30 to 60 (UDOT Geotechnical Report, 1996). Table 1 summarizes some of the engineering index properties of the Bonneville Lake deposit.

Table 1 - Summary of Soil Properties Near 100 South, I –15, UDOT Geotechnical Report, 1996

Depth (m)	Undrained Shear Strength (kPa)	Strain Compression Index	Overconsolidation Ratio
0 - 5	22 - 120	0.12 - 0.15	1.3 - 2.6
5 - 15	15 - 58	0.06 - 0.28	1.0 - 2.2
15 - 40	35 - 120	0.09 - 0.34	1.0 - 2.0

Previous observations by UDOT along sections of I-15 in the 100 South area show settlements of up to 1400 mm over 30 years for embankment heights of 6 to 10 meters. Settlements on the same order of magnitude were expected for the I-15 expansion at the 100 South utility crossing if the construction involved conventional earth fill or mechanically stabilized earth (MSE) wall embankments.

BACKGROUND AND INSTRUMENTATION

The I-15 Reconstruction at 100 South required raising and widening of the existing embankment to the limits of the right-of-way. To eliminate most of the expected settlements and related effects on existing buried utilities, EPS geofoam was selected as a super lightweight fill for the embankment widening. The geofoam fill in both the north and southbound directions was centered over a 406 mm high-pressure gas line (Figure 2). The construction was phased to allow two-way traffic at all times. The existing southbound lanes remained open while the northbound side was constructed. When the southbound lanes were under construction, the completed northbound lanes were opened for two-way traffic. The southbound portion of the embankment employed approximately 3400 m^3 of 18 kg/m^3 minimum (20 kg/m^3 nominal) density geofoam blocks, manufactured to 0.8 m X 1.2 m X 4.9 m with 0.5% dimensional and 0.5% flatness tolerances. The height of the embankment decreases southbound to conform to the longitudinal roadway grade. As shown in Figure 2, the embankment heights (not including the pavement thickness) decreases from 8.1 to 6.9 meters, corresponding to 10 to 8.5 layers of geofoam blocks, respectively. The geofoam embankment transitions to MSE wall segments on both the north and south sides. The top portion of the existing

embankment was subexcavated and replaced with scoria fill to raise the roadway grade within the utility corridor without additional loading of the compressible foundation soils.

Two sets of instrumentation array have been installed at the 100 South crossing of I-15. The arrays were installed during construction of the geofoam embankment in the Summer and Fall of 2000, with the objective of observing stresses and settlements both during and following construction. The North Array includes one basal earth pressure cell, a horizontal inclinometer below the geofoam wall, and a magnet extensometer column. The South Array consists of two basal earth pressure cells, two horizontal inclinometers (one at the base and one near the top of the geofoam), and one magnet extensometer column. Figure 3 shows the embankment cross-section at the south instrumentation array.

Total earth pressure cells of 345 kPa capacity were installed 150 mm into the bedding sand underlying the geofoam (Figure 4). Pressure readings were detected by vibrating wire transducers. The accuracy and resolution of the cell readings were +/- 0.9 and +/- 0.4 kPa, respectively. Zero readings showed one of the cells in the South Array to be non-responsive. The remaining two cells showed significant pressures with just one half-height block of foam in place. Subsequent increases in stress readings were consistent with the applied incremental load. The zero shift suggests the stress cells were overloaded during construction.

Magnet extensometers were placed through the height of the geofoam fill at both the North and South Array. The magnet extensometer consists of 33 mm inside diameter magnet core at the center of a 305 mm by 305 mm bearing area and 12.5 mm thick PVC plate. An augur with 120 mm diameter bit was used to bore through successive layers of geofoam. A schedule 40 PVC pipe passes through the magnet core of each plate to form a column. The extensometer probe detects the dead zone between the north and south poles of the magnet core as the position of the plate. Both magnet extensometer pipes were raised through the pavement section and fitted with flush-mounted monitoring well casing (Figure 5). The probe depth can be read to +/- 3 mm resolution.

The two basal inclinometers were set in the foundation soils prior to placement and leveling of the bedding sand and pouring of the grade beam for the facia wall. The lengths of the 85 mm inside diameter inclinometer casings for the North and South Array are 4.3 m and 4.9 m, respectively. Both extensometers tie into the toe of the existing embankment and terminate in access boxes outside the wall (Figure 6). The top horizontal inclinometer of the South Array is 30 m long and straddles across the geofoam and scoria fill over the existing embankment. U-shaped plywood templates of 150 mm depth were used to trace a cradle trench with a hot wire cutter. The U-trench was lined with a geotextile fabric across geofoam blocks and a thin layer of bedding sand was placed for seatng. The casing was then connected and installed in the foam U-trench, followed by backfill and leveling of hand compacted sand. The final geofoam course of half-height blocks was then placed over the U-trench. The horizontal inclinometer was extended in 3.05 m lengths into the scoria fill to monitor transitional settlements between the reconstructed and existing embankments. The horizontal inclinometer probe has an accuracy of +/- 0.24 mm/m, and a resolution of +/- 0.04 mm/m.

Thermistors were later installed in both the geofoam treated and conventional fill embankment locations. These sensor columns were installed late in 2001 and readings have not been obtained over a winter cycle. Details of the thermistor installation and observations will be included elsewhere.

DESIGN CONSIDERATIONS

The construction of geofoam embankments can be successfully completed without triggering primary consolidation as well as excessive secondary compression of foundation soils. A volume of soil approximately equal to the load produced by adding the widened embankment was excavated, providing a “zero net load” on the subsurface. Type VIII geofoam (ASTM C-578) blocks of 18 kg/m^3 minimum density were installed as manufactured. A series of laboratory tests confirmed the density of geofoam supplied to the I-15 project exceed the minim specified density and the average compressive strength at 10% strain was 111 kPa and was also higher than the minimum of 90 kPa given by ASTM-C-578. A design working stress of 30% for dead load and up to 10% of the compressive resistance due to live load was allowed. This criterion was selected to limit the long-term creep deformation of the geofoam fill to no more than 2% over 50 years. The corrected modulus to 1% strain obtained from the laboratory tests were in the range of 2.9-5.1 MPa. The laboratory tests used from 50 mm cube samples and

loading was at 10% strain per minute; as per ASTM-D-1621. Further tests on large samples indicate significant size effects and that the design values obtained for 50 mm samples are conservative (Elragi, et al, 2000).

LOAD HISTORY

The load history at 100 South is shown in Figure 7. Geofoam placement started on 21 July and was completed by 4 August, 2000. Placement of 610 mm course of 8.8 kN/m^3 compacted density scoria and the 460 mm course of 21 kN/m^3 open graded sub-base was finished on 29 August 2000. Construction at 100 South resumed with the pouring of the PCC Pavement on 15 March 2001. The load exerted by the pavement section represents the design working stress due to dead weight for the geofoam fill. Jersey barriers were installed on 3 May 2000, and planter boxes and sound barrier walls were placed on 12 May 2001. Figure 7 shows the time history of the north and south basal stress cell readings and estimated stresses based on the thickness and assumed densities for the different layers. The three curves are in reasonably good agreement. Allowing for the initial zero shift of the stress cells, pressures registered by the stress cells are below the allowable working stress and calculated estimates. The sound and traffic barrier loads contribute to a localized stress increase above that due to the standard pavement sections. Similar base stress cells at 3300 South register less pressure than stress cells at 100 South (Bartlett, et al, 2001).

SETTLEMENT OBSERVATIONS

Vertical movements within the geofoam fill are observed by extensometer readings that are referenced to the base plate. Figures 8 and 9 show the cumulative geofoam block settlement with time for the north and south array together with the load history. With placement of the load distribution slab, settlements of 3 and 5 mm for the bottom blocks to 19 and 23 mm for the overall mass of geofoam were observed, for the north and south array, respectively. As the compacted scoria and open graded base was placed, the geofoam mass once again began to settle, and additional vertical deformations of about 15 mm and 58 mm developed for the bottom and the overall geofoam mass, respectively.

Over the construction rest period of more than 100 days preceding the installation of the PCC pavement, settlement eased. In fact, an upward movement was recorded for the entire South Array, and also for the top three cumulative sample points in the North Array. This movement, observed in both magnet extensometer arrays, was coupled with stress reductions in both basal stress cells. The construction method with geofoam, provided full load compensation and no net stress was applied to the foundation soils. By subexcavation and replacement with scoria fill, the adjacent MSE wall segments were load compensated and should not be undergoing primary consolidation settlement. However, the net loading in the geofoam area is much less than at MSE wall segments. The 8-meter MSE walls and transition to the geofoam continue to settle gradually in secondary consolidation. Geofoam blocks were installed with staggered vertical joints and appear to react as a beam in rebounding, and providing a protective "arch" around the 406 mm high-pressure gas line in response to larger settlements in the MSE area. When construction resumed, and the PCC pavement was poured over the load distribution slab and road base, the geofoam embankment settled in response to the load addition. Similarly, movement continued as the jersey barrier and planter box was poured, and filled. Total vertical movements to date, comprised of both compressive deformation and seating, reached about 85 mm, for both the north and south arrays. If indeed the postulated arching of the geofoam fill holds true, the noted stress reduction and sense of movement should be repeated. Vertical deformations tend to cease as block seating and gap closure progressed following application of each load increment. The settlements at 100 South are in good agreement with those observed at 3300 South (Bartlett, et al, 2001).

Figures 10 and 11 show height differences between magnetic plate separations and the nominal thickness of blocks confined between the plates. The height difference, $\mathbf{h_d}$, between magnet extensometer plates at any time is given by:

$$\mathbf{h_d = H_{12} - [(d_2 - d_1) - t_p]}$$

Where:
- $d_{1,i}$ = depth to magnet plate 1
- $d_{2,i}$ = depth to magnet plate 2
- $H_{12,i}$ = nominal height of geofoam blocks between magnet plates 1 and 2
- t_p = thickness of one magnet plate, 12.5 mm

The dimensional tolerance allows for +/- 4 mm for each block and represents error when computing the amount of gaps. There may also be slight deviation in the verticality of the 25 mm riser pipes, but as the riser pipes do not carry load, this is assumed to be negligible. Elragi (2000) suggested that positive values returned on the gap computation, neglecting the thickness of the plate, were due to the dimensional tolerances. However, this only allows up to +/- 8 mm in height between two full height blocks and the measurement interval.

The initial, or zero reading of the magnet extensometer arrays at 100 South show some layers with negative height differences. Allowing for the pressure of magnet plates between layers and without considering flatness error of less than 25 mm, the error in the measured height difference would vary between +/- 11 mm (for a two block measurement interval). In general, with increases in load, gaps close and blocks deform to result in height differences. Negative height differences at the end of construction suggested that gaps still remained for some layers. Within the resolution of the magnet extensometer probe all movements diminish with the end of construction.

The two basal and one top horizontal inclinometers at 100 South record the cross-sectional embankment settlement, as shown in Figures 12, 13, and 14. The basal inclinometer data show the settlement response of the foundation soils below the geofoam. More settlement occurred during construction beneath the grade beam supporting the wall than below the geofoam. With time, further settlement followed in parts of the foundation underlying the geofoam. The foundation settlement below the grade beam at both basal inclinometers is about 80 mm. Settlements beneath the back end of the inclinometers have reached 80 and 70 mm for the north and south array, respectively. Settlement rates were higher beneath the grade beam initially, but are now higher at the back. This suggests a higher rate of deformation beneath the old embankment and raised grade achieved with the scoria fill. The most recent readings indicate gradual differential settlement of up to 0.1 mm/day over the length of each inclinometer.

The subsurface reaction to the placement of the load slab on 14 August 2000 was more evident at the grade beam. The addition of the scoria, open graded base, PCC pavement, and detailing, led to more settlements, with sustained rates on the order of 0.2 – 0.3 mm/day. A subsequent reading on 18 September 2001 of the basal inclinometer at the south array, however, shows the post construction rate of settlement slowing to approximately 0.1 mm/day. Subsequent readings of the basal inclinometers should indicate slowing of settlements. Overall, the basal inclinometers show a total of about 80 mm of foundation soil settlement under the geofoam by the end of construction.

The data for the top inclinometer at the south array shows the performance of the geofoam and scoria fill. The fascia wall and full geofoam section have experienced a total settlement of about 150 mm. In the transition zone, total settlements vary between 150 and 200 mm. Almost 250 mm settlement has taken place beneath the roadway centerline and scoria fill segment. At present, the rate of settlement is about 0.3 mm/day at the wall face and approximately 0.4 mm/day at the road centerline in the scoria fill section. The settlement across the inclinometer profile is relatively uniform. Both incremental and differential settlements have been decreasing. The difference in total settlement between the basal and top inclinometers of about 80 mm match the total settlements shown in the magnet extensometer data.

Figure 15 presents average stress-strain curves derived from stress cell and extensometer deformation increments, neglecting stress due to the self-weight of the geofoam fill and the initial zero shift of the stress cells. The initial segments of the curves manifest a similar deformation to seating error in small test sample data as represented by the uncorrected stress-strain curve for a standard compression test on a 50 mm cube sample. The global stress-strain curves of the geofoam are for layer 1.5 to layer 9.5 and 9 for the north and south arrays, respectively. The trends of the three curves are similar. As the loading is increased, seating and gap closure occurred. The modulus gradually increased. Corrected modulus (ASTM D-1621) values for Type VIII geofoam, used for the I-15 project, determined from 50 mm samples were on the order of 2.9 to 5.1 MPa. The provisional GRC geofoam specifications provide a modulus to 1% strain of 4.3 MPa for the Type VIII geofoam. BASF Corp. (1998) indicates the modulus of EPS 20 falls in the range of 3.4 to 7.0 MPa. The trend of field moduli beyond the installation of the load distribution slab are of the order of 10 MPa and higher than values from standard small sample lab tests. Deformations of the geofoam fill due to seating and gap closure take place during construction and before final paving. The response of the pavement under service loads and the performance of the geofoam fill would be assessed to be inferior if the evaluation is based on small sample laboratory tests. This conclusion is

supported by a number of research findings. A constitutive model based on the parameters derived from small sample tests overestimated the deformation of a model embankment (Frydenlund and Aabøe, 1996). Results from 50 mm and 0.6 m cube samples show the large samples result in much higher modulus for the same density geofoam. Elragi (2000) and Elragi et al, (2000) find the modulus of EPS to be proportional to density, for a given sample size, and report a modulus of about 10 MPa for EPS 20. Duskov (1997) used a falling weight deflectometer to back calculate the modulus values for EPS 20, EPS 25, and EPS 30 from both test pavement sections as well as constructed embankments. The range in moduli for EPS reported from these exercises is 10 to 34 MPa. Sivathayalan, et al., (2001) indicate the initial modulus for Type VIII geofoam would be on the order of 20 MPa based on a wave propagation method of determination. Negussey et al, (2001) report modulus values higher than 10 MPa based on yet another method of assessment, flexure tests as per ASTM-C-203 on Type VIII geofoam. These recent findings and the field observations at I-15 suggest that small sample modulus values for geofoam be used more as a common index rather than for analysis and design directly. Making use of the linearity between modulus and density for all sample sizes (Elragi, 2000; Elragi et al, 2000), modulus values derived from small samples can be adjusted by multiplying by a factor of 2 to 3 to obtain appropriate design values for geofoam. The amount of deformation that occurs during construction as a result of seating and gap closure can be minimized by tighter control of dimensional tolerances and careful installation practice. These settlements were compensated during construction at I-15 and the added effort and cost of trimming individual blocks to achieve tight closure was not necessary.

SUMMARY AND CONCLUSIONS

Geofoam was used for the I-15 Reconstruction to successfully reduce settlements. Field data collected during and after construction validated the design assumptions. Stress cell indicate gradual adjustment, as gaps close and blocks seat. The construction rest period as well as the end of construction settlements show the geofoam fill tends to form a protective arch over critical utilities as adjacent MSE fill segments settle in secondary compression. Inclinometer data further show the effectiveness of geofoam for challenging embankment widening applications. Modulus estimates from the field data support previous and ongoing findings that small sample test results should be adjusted to better predict in service performance.

ACKNOWLEDGEMENTS

The authors would like to thank the Utah Department of Transportation for providing the internship leading to research efforts presented in this paper; Huntsman Chemical Corp., for funding in part the research at the Geofoam Research Center; Huang Xiadong for help with the figures; and undergraduate research assistants at the University of Utah.

REFERENCES

Bartlett, S., Negussey, D., Kimble, M., Sheeley, M., 2000, Use of Geofoam as a Super-Lightweight Fill for I-15 Reconstruction, Presentation at Transportation Research Board 79th Annual Meeting, Washington, D.C.

Bartlett, S., Farnsworth, C., Negussey, D., Stuedlein, A., 2001, Instrumentation and Long Term Monitoring of Geofoam Embankments, I-15 Reconstruction Project, Salt Lake City, Utah, EPS Geofoam 2001, 3rd International Conference on EPS Geofoam, Salt Lake City, UT

BASF Corp., 1998, Styropor Technical Information, Technical Information, BASF Corp., Germany

Duškov, M., 1997, EPS As A Lightweight Sub-base Material In Pavement Structures, Ph.D. Dissertation, TU Delft, Netherlands

Elragi, A.F., 2000, Selected Engineering Properties and Applications of EPS Geofoam, Ph.D. Dissertation, State University of New York College of Environmental Science and Forestry, Syracuse, NY

Elragi, A. F., Negussey, D., Kyanka, G., 2000, Sample Size Effects on the Behavior of EPS Geofoam, Soft Ground Technology Conference, Noordwijkwehout, The Netherlands

Frydenlund, T.E., and Aabøe, R., 1996, Expanded Polystyrene – The Light Solution, Proceedings of the International Symposium on EPS Geofoam, Tokyo

Negussey, D., Anasthas, N. and Elragi, A. F., 2001, Young's Modulus of EPS Geofoam by Simple Bending Test, EPS Geofoam 2001, 3rd International Conference on EPS Geofoam, Salt Lake City, UT

Sivathayalan, S., Negussey, D. and Vaid, Y. P., 2001, Simple Shear and Bender Element Testing of Geofoam, EPS Geofoam 2001, 3rd International Conference on EPS Geofoam, Salt Lake City, UT

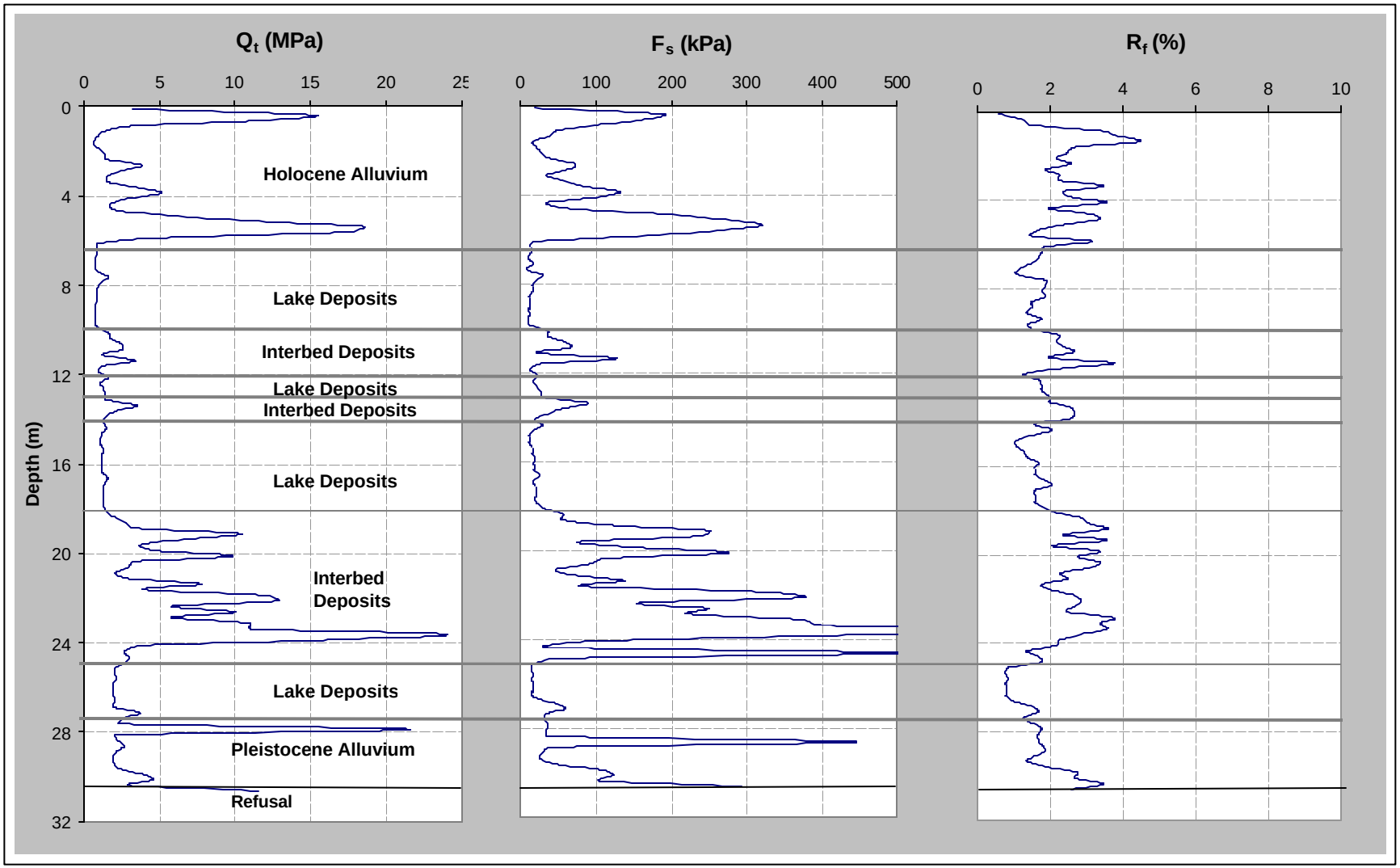

Figure 1 – Soil profile from CPT sounding 06-SC-10 near 100 South geofoam array site (UDOT Geotechnical Report, 1996).

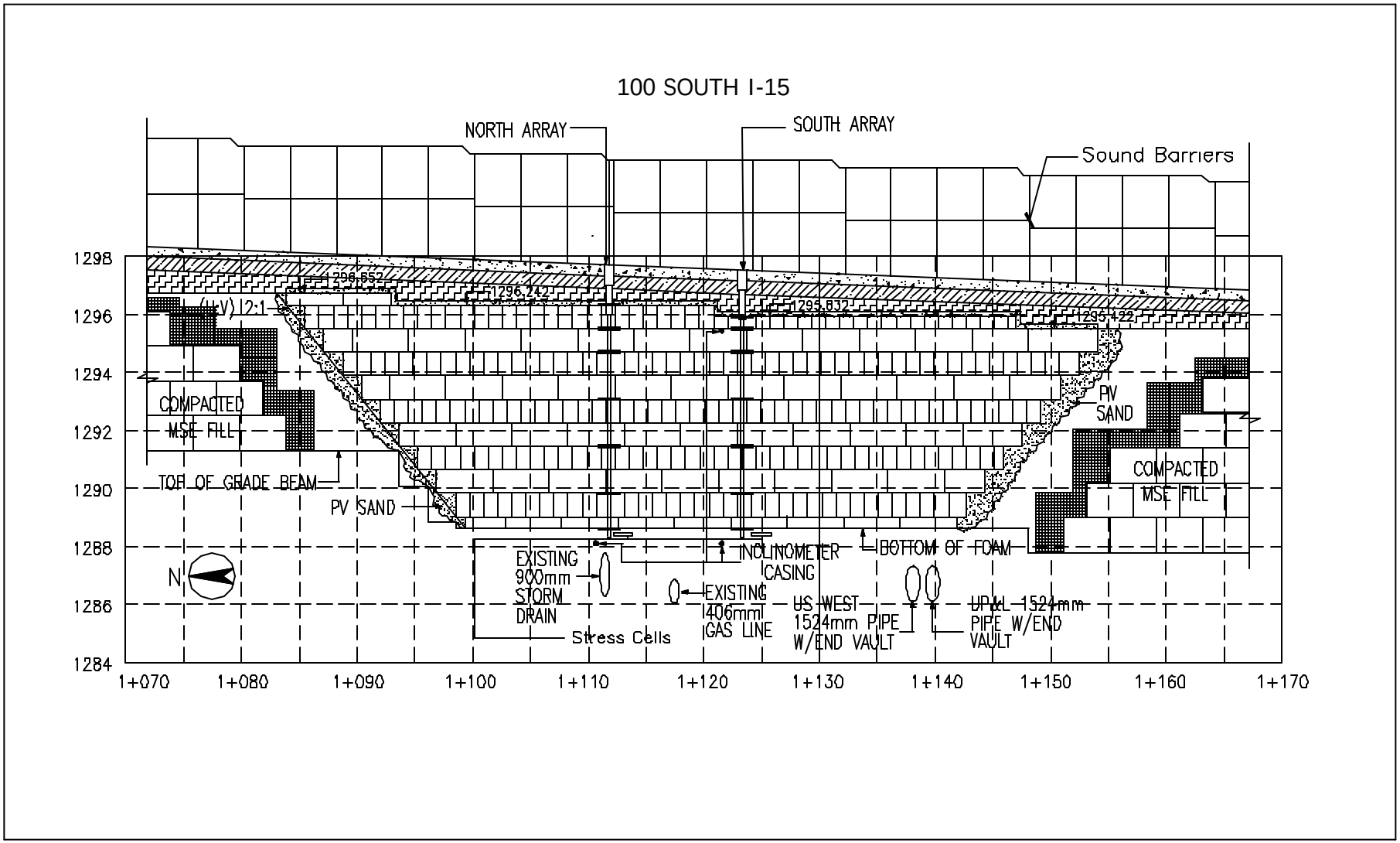

Figure 2 – Elevation View of I-15 Southbound at 100 South looking east.

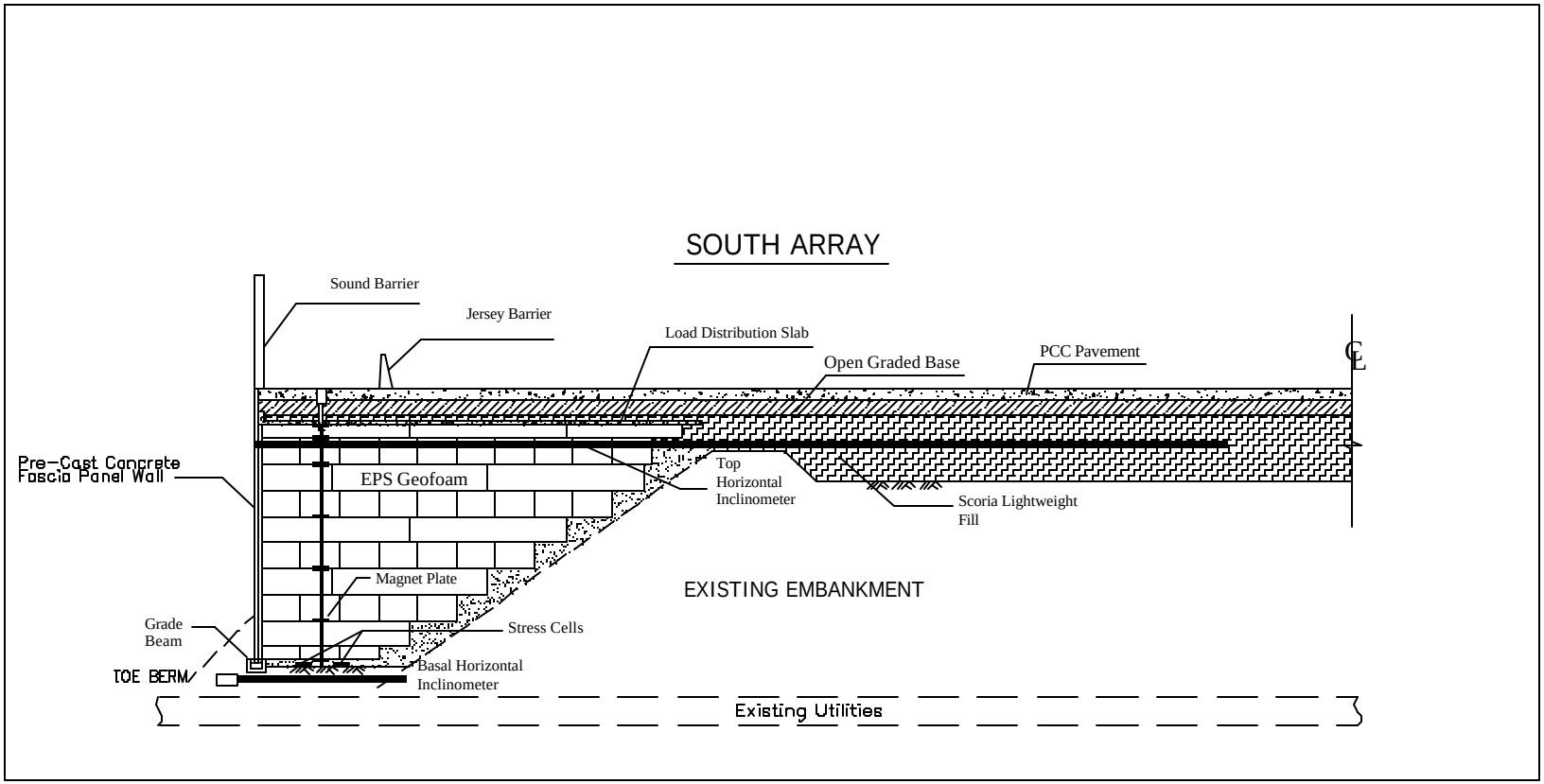

Figure 3 – Section profile of I-15 Southbound at 100 South showing south instrumentation array, looking north.

Figure 4 – Stress cell and extensometer plate in the leveling course below the geofoam fill. Note geofoam and grade beam for fascia wall support in background.

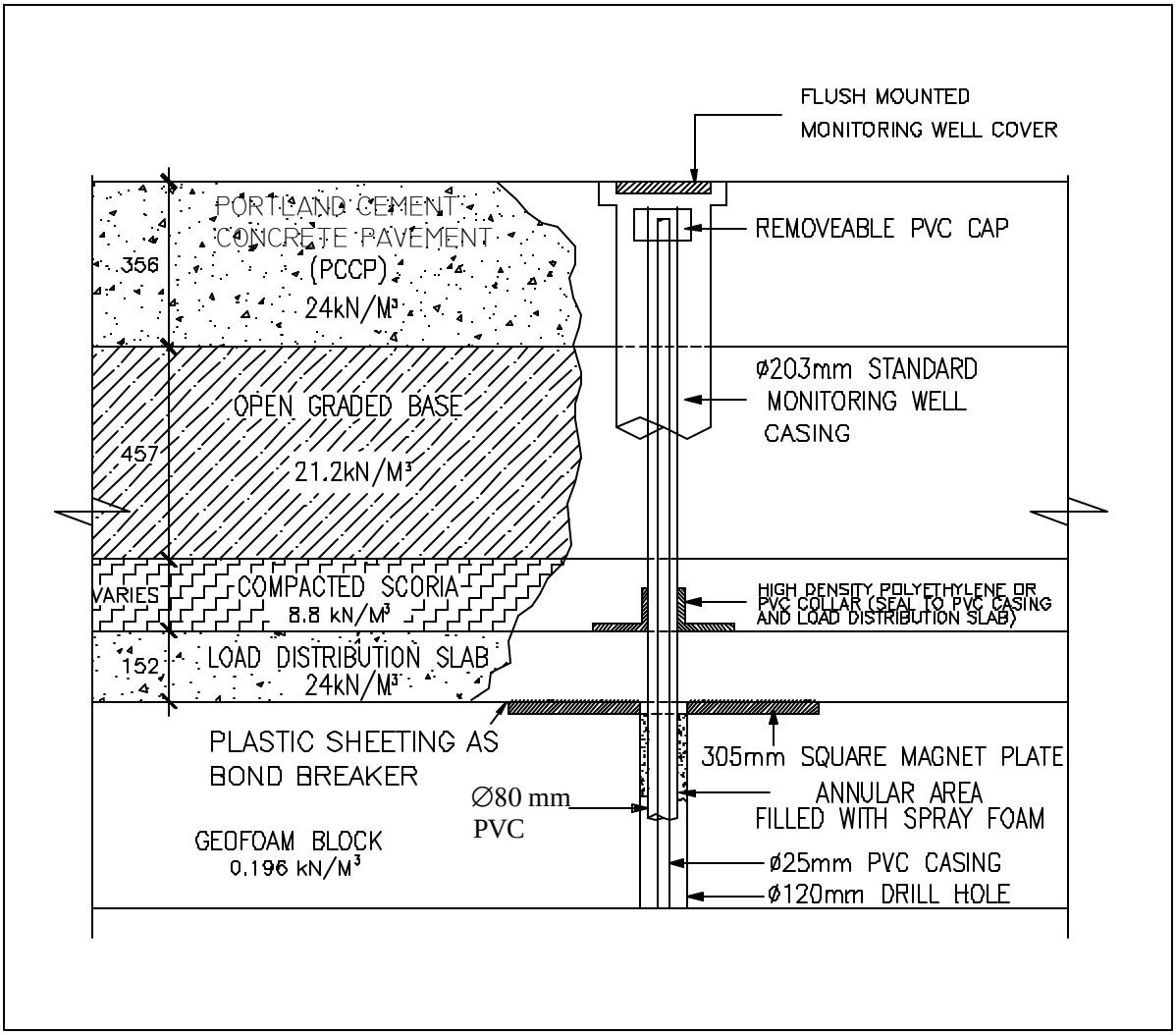

Figure 5 – Extensometer completion details.

Figure 6 – Access port for the north array basal inclinometer beneath the fascia wall grade beam (See Figure 3).

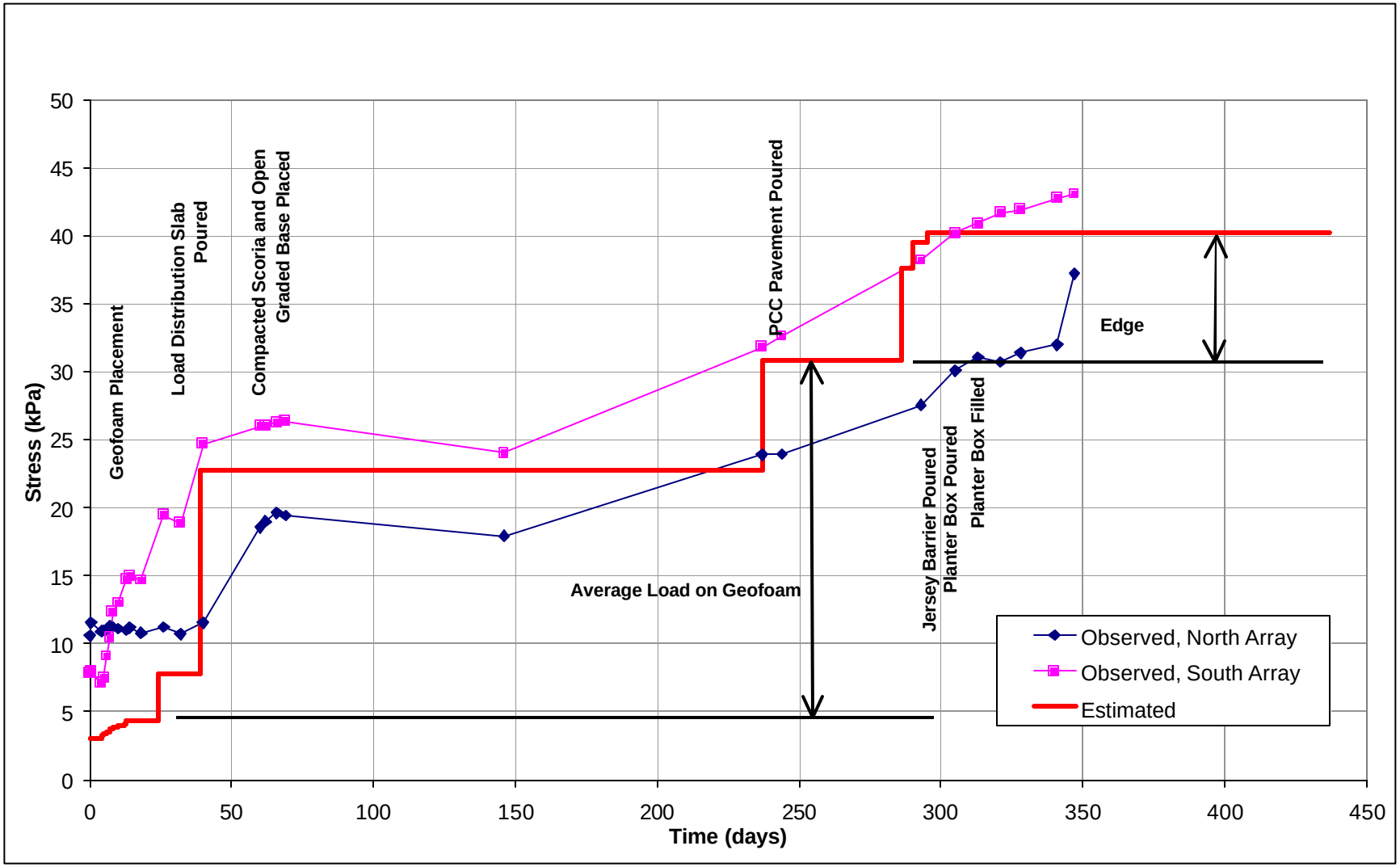

Figure 7 – Observed and estimated load histories at 100 South.

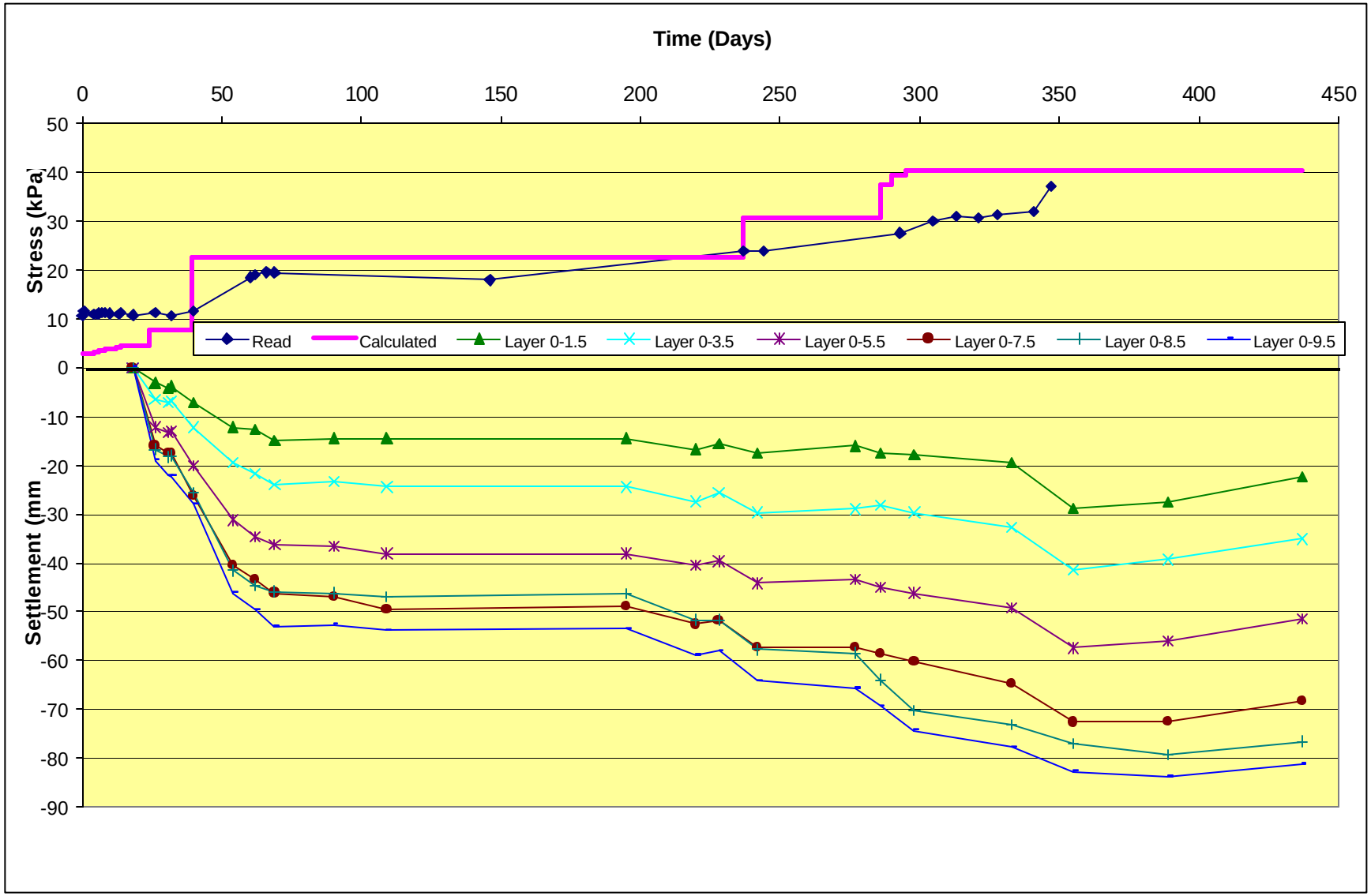

Figure 8 – Extensometer settlement history for the north array at 100 South.

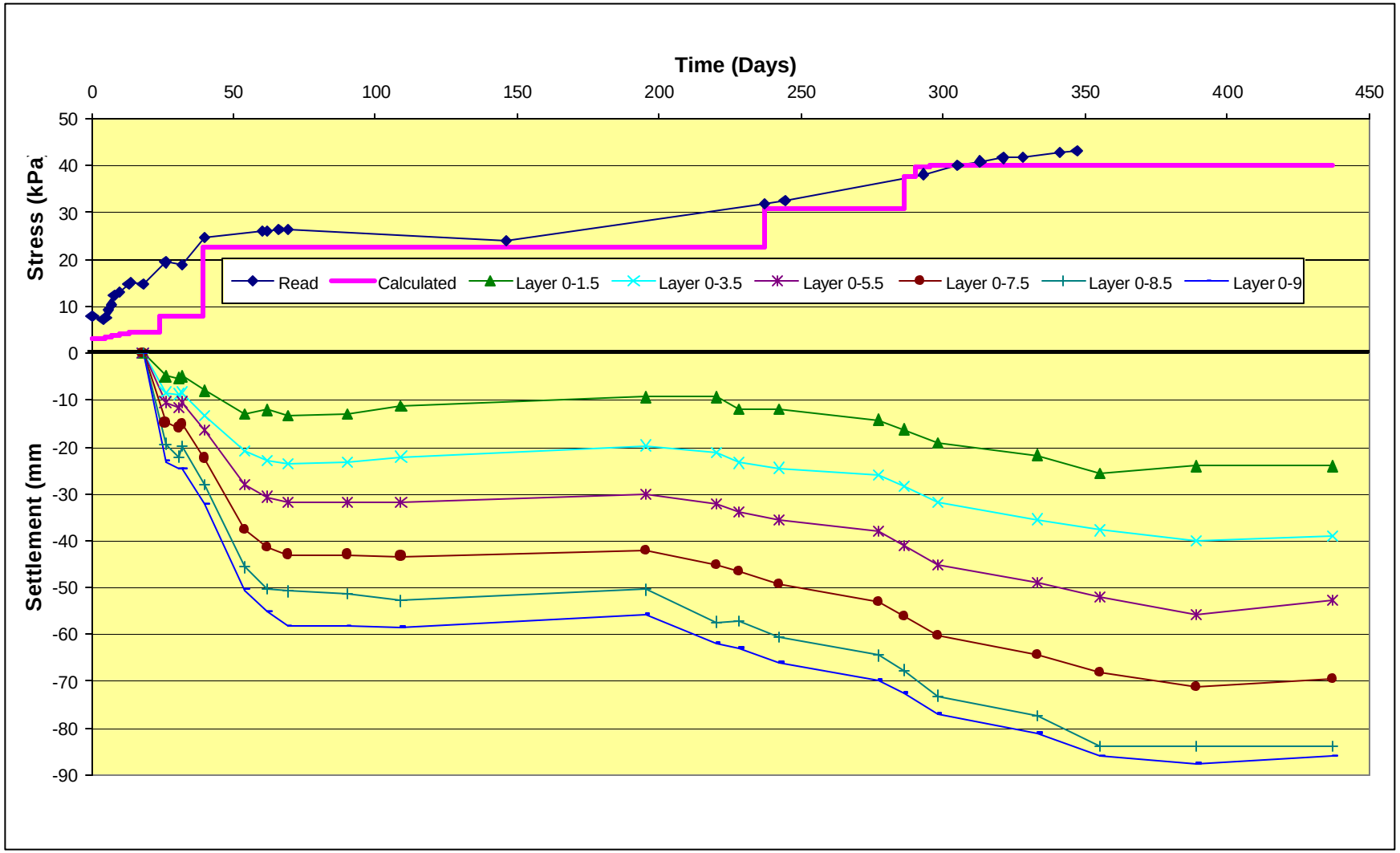

Figure 9 – Extensometer settlement history for the south array, 100 South.

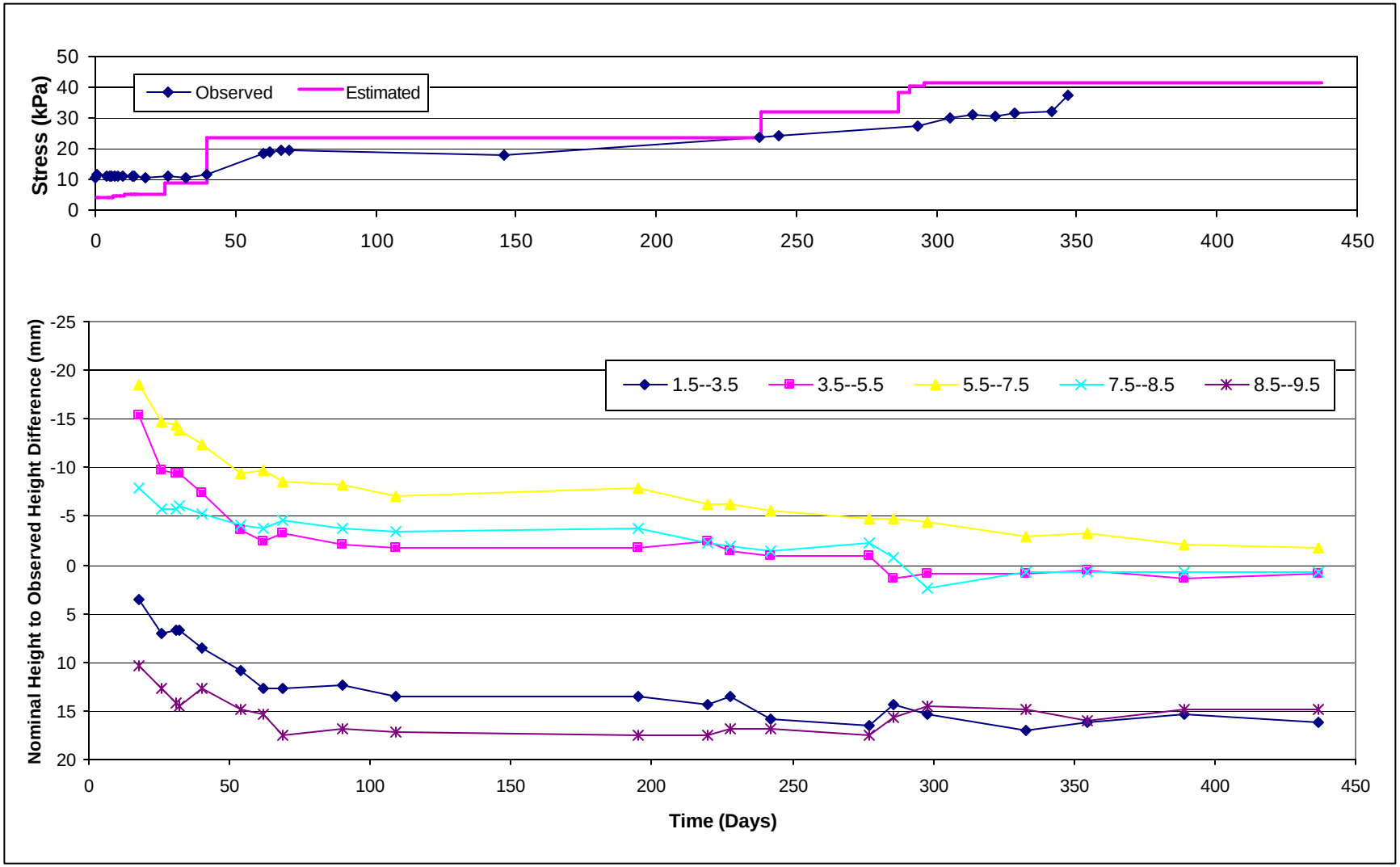

Figure 10 – Extensometer height difference history at the north array, 100 South.

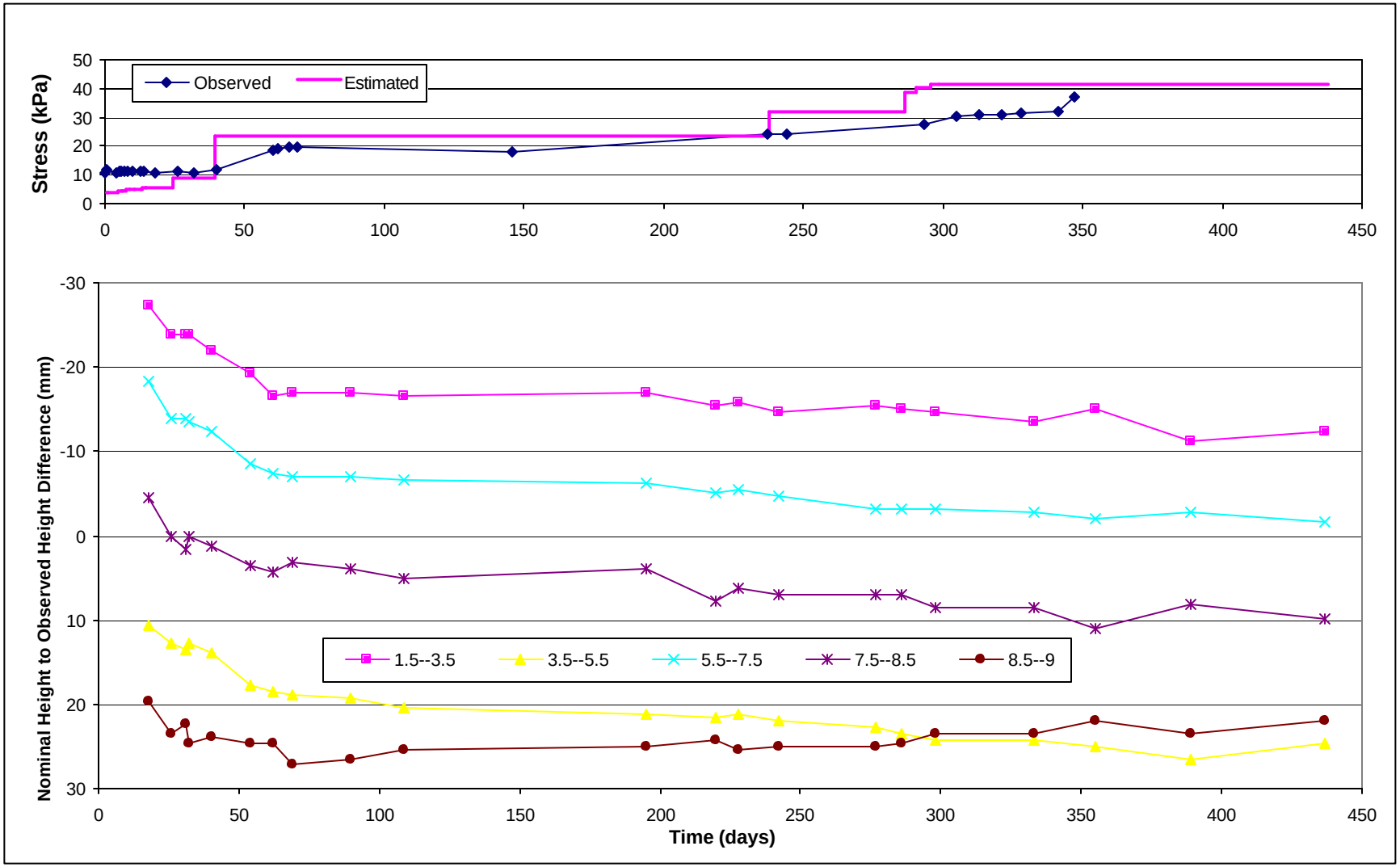

Figure 11 – Height Difference history at the south array, 100 South.

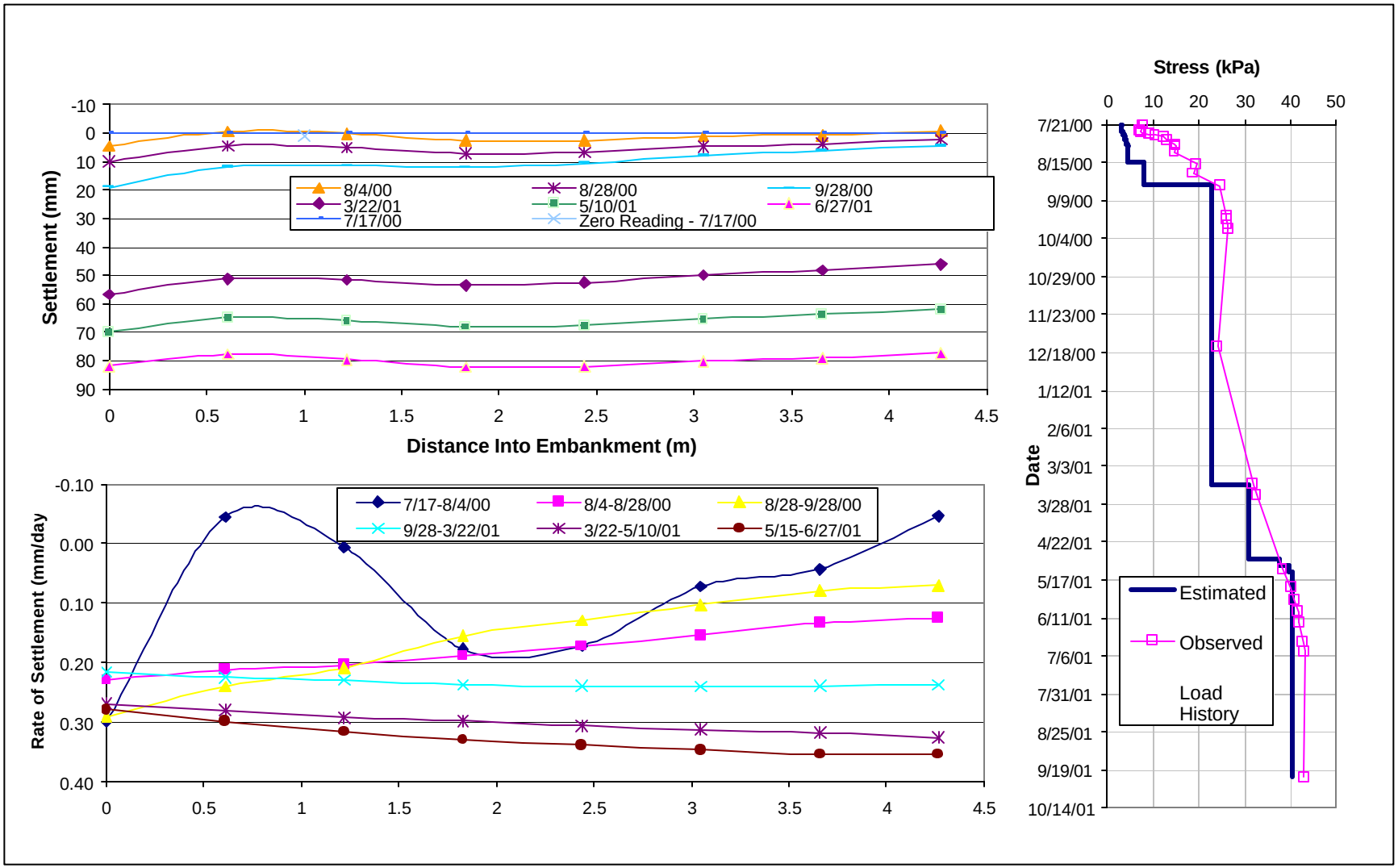

Figure 12 – Basal cross-section settlement at the north array, 100 South.

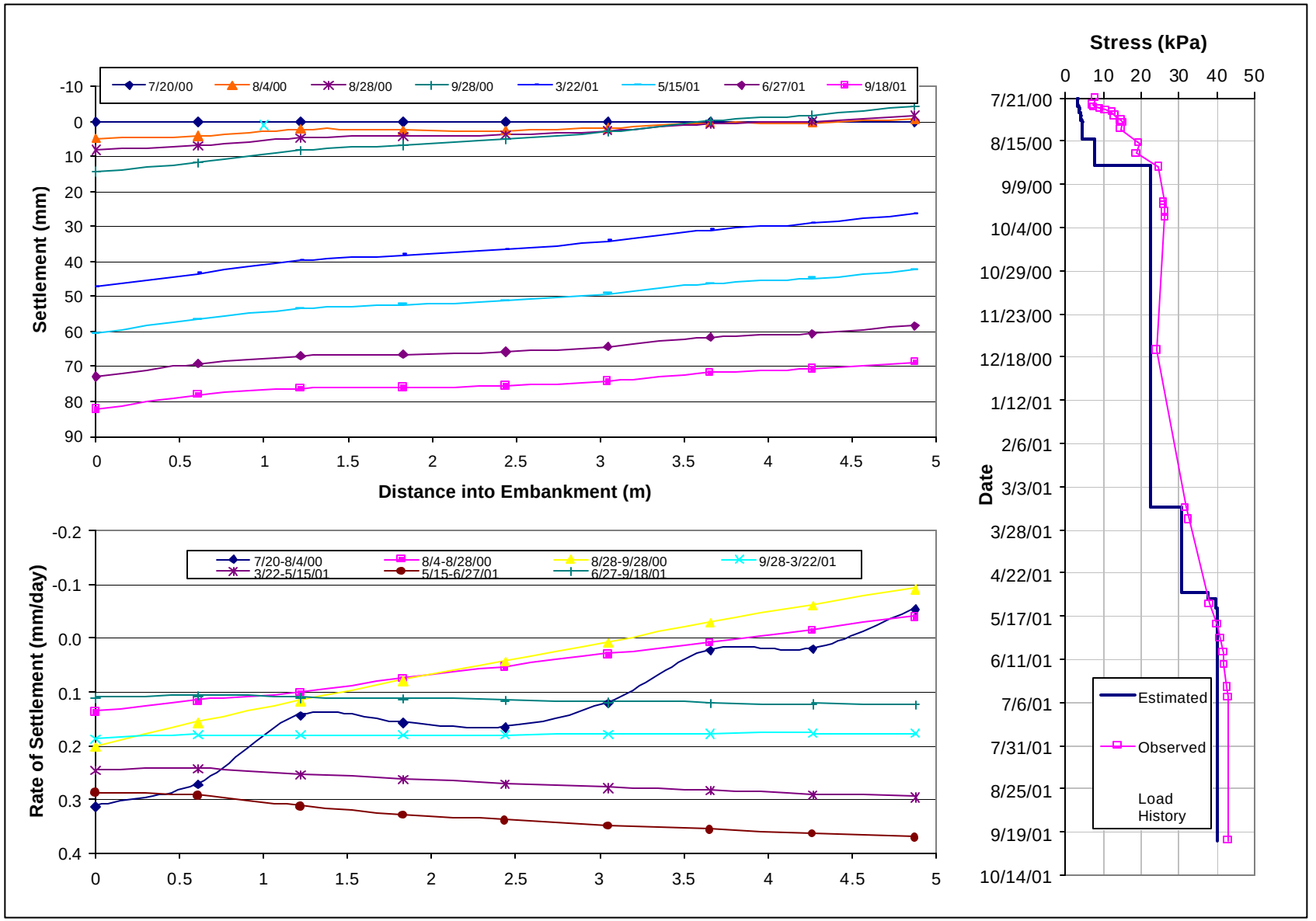

Figure 13 – Basal cross-section settlement at the south array, 100 South.

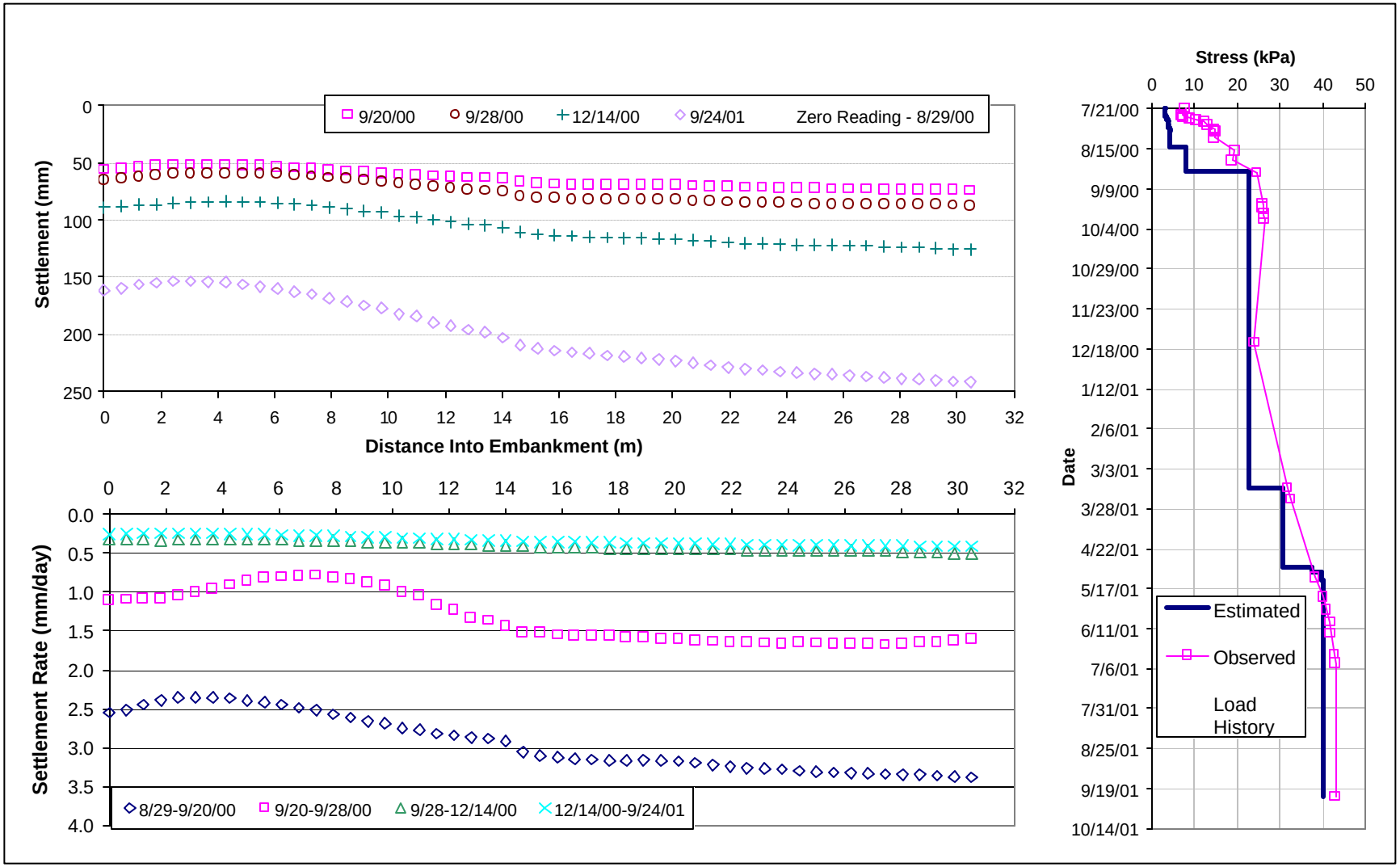

Figure 14 – Top cross-section settlement at the south array, 100 South.

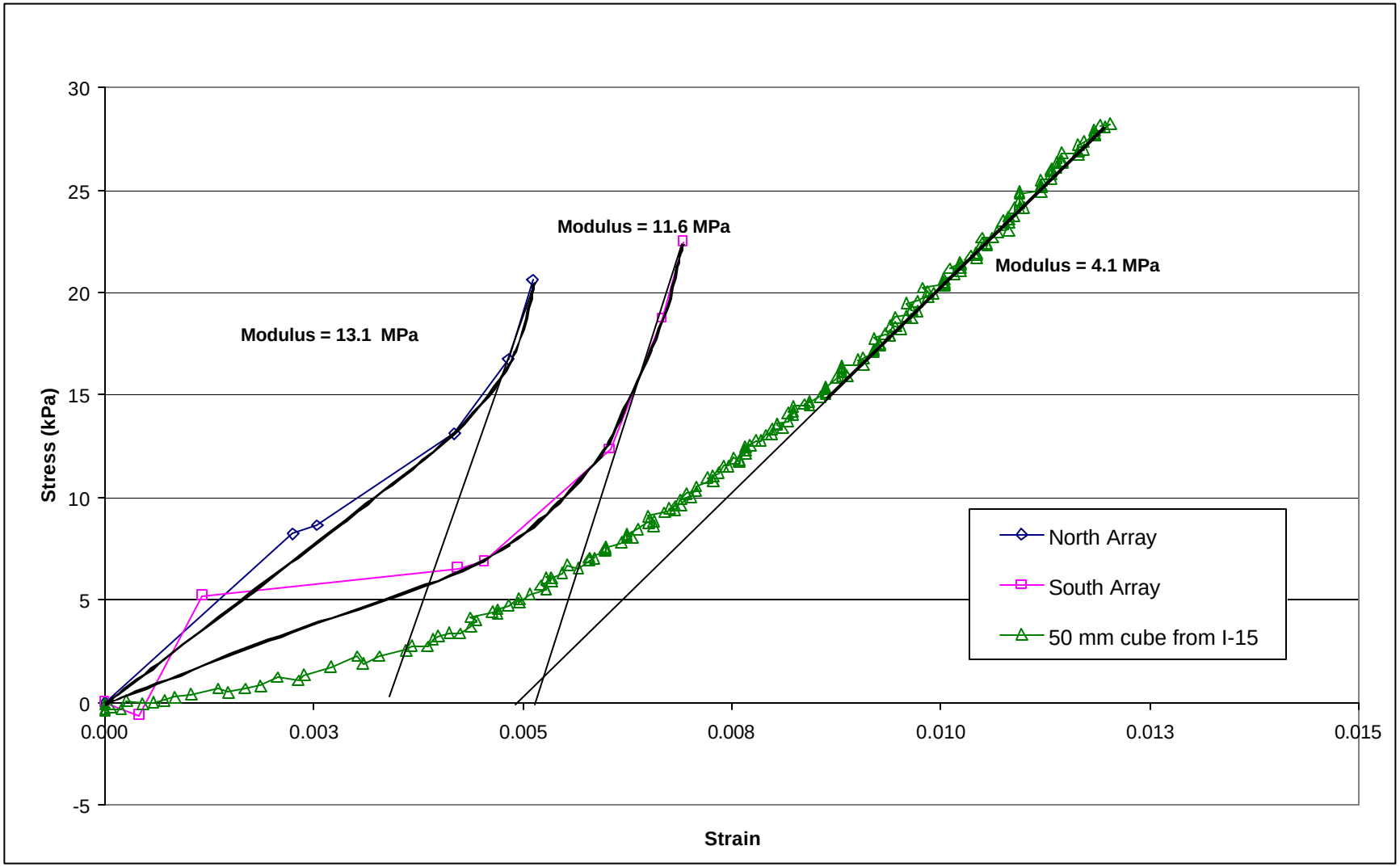

Figure 15 – Average stress-strain curves derived from stress cells and extensometer increments.